DALTON

Intramolecular competition between histidine and methionine side chains in reactions of dipeptides with $[Pt(en)(H_2O)_2]^{2+}$ (en = $H_2NCH_2CH_2NH_2$)

Christian D. W. Fröhling and William S. Sheldrick *

Lehrstuhl für Analytische Chemie, Ruhr-Universität Bochum, D-44780 Bochum, Germany

The pH- and time-dependent reactions of $[Pt(en)(H_2O)_2]^{2+}$ (en = $H_2NCH_2CH_2NH_2$) with the histidylmethionine dipeptides cyclo(-his-met-), his-Hmet and met-Hhis at 313 K have been studied by ion-pairing reversed-phase HPLC and ^1H and ^{195}Pt NMR spectroscopy. Quantitative formation of the unusually large 12-membered chelate ring in the remarkably inert complex $[Pt(en)\{cyclo(-his-met-)\}]^{2+}$ is complete within a few minutes. A base-catalysed configuration inversion for one of the diketopiperazine α-C atoms at pH > 9 leads to the observation of two well separated HPLC fractions for both the prevailing $\kappa^2N'_{met},S$ co-ordinated species and the peptide itself. An analogous likewise kinetically stable macrochelate is present after 14 d as a major species in the $[Pt(en)(H_2O)_2]^{2+}$–his-Hmet reaction mixture over the whole range 3.2 < pH < 11.2. Time-dependent HPLC indicated that a kinetically favoured κ^2O,S chelate is rapidly formed at pH 4.55 only slowly to convert into competitive S-bound complexes with κ^2N^1,S and $\kappa^2N'_{met},S$ co-ordination. After reaching a quasi-stationary state (50 h), amide N'_{met} anchoring in the latter species facilitates co-ordination of the adjacent amino nitrogen to afford the thermodynamically preferred κ^2N (amino),N'_{met} chelate. At a 2:1 molar ratio, slow reaction of the macrochelate with a second $(en)Pt^{II}$ fragment led to formation of $[\{Pt(en)\}_2(his{H}_{-1}\text{-Hmet-}1\kappa^2N,N^3:2\kappa^2N^1,S)]^{3+}$. In met-Hhis, κ^2N (amino),S chelation is kinetically and thermodynamically preferred in acid solution. At pH 9.6, however, sulfur binding is thermodynamically unfavourable, and the initially formed κ^2N (amino),S complex slowly converts into a κ^2N (amino),N'_{his} species, which subsequently affords $[Pt(en\text{-}\kappa N)\{met\text{-}his\text{-}\kappa^3N$ (amino),$N'_{his},N^3\}]^+$ on cleavage of the Pt–N (en) bond *trans* to the amino N atom.

It is generally accepted that DNA co-ordination at guanine N^7 is of key importance in the mechanism of action of platinum anticancer drugs such as cisplatin, *cis*-$[PtCl_2(NH_3)_2]$.[1,2] However, Pt^{II} is known to exhibit a high kinetic affinity for sulfur-containing ligands[3] and the concentration-dependent nephrotoxicity of cisplatin has been ascribed to its reaction with L-cysteine or L-methionine (Hmet) side chains in certain enzymes.[4] One of the few characterized metabolites of cisplatin is indeed the bis-chelate $[Pt(met\text{-}\kappa^2N,S)_2]$, which has been isolated from the urine of chemotherapy patients.[5] Recent reports[6,7] of the replacement of a thioether S by a guanine N^7 in the square-planar co-ordination sphere of the model fragment $[Pt(dien)]^{2+}$ (dien = diethylenetriamine) have also provided support for the concept of a platinum-pool mechanism in which initial kinetically favoured protein binding may provide a route to DNA platination. Of interest in this context, is the observation that the rate of reaction of cisplatin with guanosine 5′-monophosphate (5′-GMP) increases in the presence of Hmet owing to the labilization of an ammine ligand in the κ^2N,S co-ordinated intermediate $[Pt(met\text{-}\kappa^2N,S)(NH_3)_2]^+$ as a result of the high *trans* effect of the thioether sulfur.[8] An *in vivo* investigation has demonstrated that such chelates, present in a cisplatin–Hmet (1:5) mixture held for 24 h at 310 K, still exhibit significant cytotoxicity, in the absence of typical cisplatin-associated renal toxicity.[9]

Such findings have prompted recent systematic studies on the reactions of $[Pt(en)(H_2O)_2]^{2+}$ and $[Pt(en)(Me\text{-}mal\text{-}\kappa^2O,O')]$ (en = ethane-1,2-diamine, Me-mal = 2-methylmalonate) with methionine-containing peptides such as L-methionylglycine (met-Hgly) and glycyl-L-methionine (gly-Hmet);[10,11] en was employed as a less readily displaced chelating ligand to avoid the complications in reaction behaviour caused by the facile release of ammine ligands sited *trans* to methionine S in products formed by cisplatin itself. In view of the known high affinity of Pt^{II} for *softer* ligands, it is somewhat surprising that remarkably few reports of the interaction between platinum (or palladium) complexes with histidine-containing peptides have appeared. The hetereocyclic imidazole ring system in the histidine side chain provides an ambidentate ligand with two competitive donor atoms. Although N^3 will clearly be preferred when the formation of small chelate rings is possible[12] as in $[PdCl(gly\text{-}his\text{-}\kappa^3N,N',N^3)]$ (N = amino, N′ = amide), monodentate co-ordination is also observed at the sterically more open N^1 site.[13] Solution studies with complexes such as $[Pt(dien)(H_2O)]^{2+}$ and *trans*-$[Pt(NH_3)_2(mgua)(H_2O)]^{2+}$ (mgua = 9-methylguanine) have confirmed the formation of both N^1 and N^3 linkage isomers.[14,15] Parac and Kostic[16] have recently demonstrated that the histidine residue serves as an anchor for the *cis*-$[Pd(en)(H_2O)_2]^{2+}$-catalysed cleavage of the peptide linkage in his-Hgly and ahis-Hgly (N-acetyl-L-histidylglycine). Although both N^1 and N^3 co-ordinated species could be detected, selective methylation of the imidazole nitrogen atoms indicated that only the N^3-bound catalyst can effect the hydrolysis.

The structural and mechanistic importance of histidine residues in protein chemistry has now led us to extend our HPLC and NMR studies[10] of the reaction of $[Pt(en)(H_2O)_2]^{2+}$ with small peptides to cover cyclo(L-histidyl-L-methionine) [cyclo(-his-met-)], L-histidyl-L-methionine (his-Hmet) and L-methionyl-L-histidine (met-Hhis). In view of the well documented kinetic preference of Pt^{II} for met S,[3,17] we have complemented the determination of species distribution diagrams in the range 3 < pH < 11 with time-dependent chromatographic analyses of binding competition between the histidine and methionine side chains.

Results and Discussion

Freshly mixed $[Pt(en)(H_2O)_2]^{2+}$–dipeptide reaction solutions for pH-dependent studies were brought immediately to the desired pH by addition of HNO_3 or NaOH. After incubation for 14 d at 313 K and subsequent registration of the final pH, such solu-

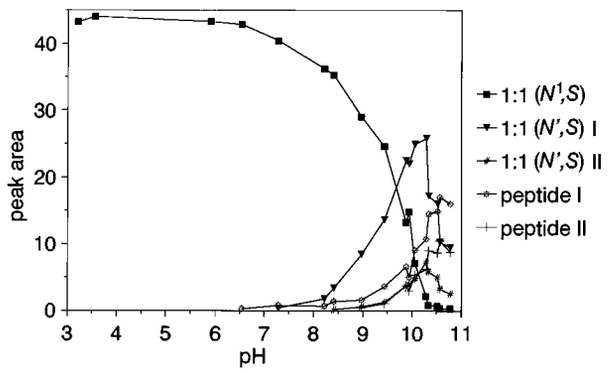

Fig. 1 Species distribution for the 1:1 $[Pt(en)(H_2O)_2]^{2+}$–cyclo(-his-met-) reaction system after 14 d at 313 K as determined by HPLC (conditions as for Fig. 4) for the range 3.2 < pH < 11.2

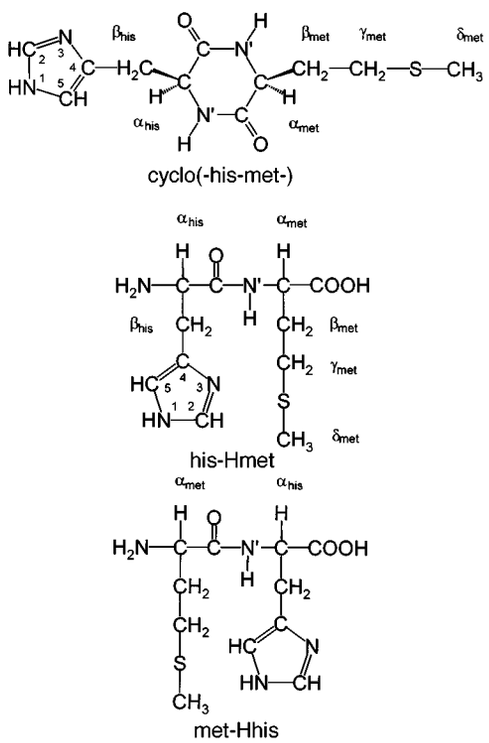

tions were held at 277 K prior to analytical or semipreparative separation by reversed-phase HPLC in the presence of the ion-pairing agent pentafluoropropionic acid (PFP). The composition of solutions was found to remain constant at this temperature over a period of several months. In the case of time-dependent investigations, HPLC separations were carried out after analogous incubation at 313 K for specified intervals. When analytical chromatograms confirmed the presence of only one major product, reaction solutions were prepared at the appropriate pH* (pH meter readings uncorrected for deuterium isotope effects in D_2O) for direct NMR measurements. As a result of the kinetic inertness of platinum(II) complexes and the relatively short retention times typically involved for HPLC separations (t_R < 45 min), elution of the reaction mixture at ambient temperature and pH 2.1 does not lead to significant changes in species concentrations. This means that both the pH and time dependences of species distribution can be monitored for $[Pt(en)(H_2O)_2]^{2+}$–dipeptide reaction systems by HPLC,[10,18] as illustrated for cyclo(-his-met-) in Fig. 1. In this diagram the ordinate gives the peak area for a particular complex at the detection wavelength of 220 nm. Knowledge of the individual absorbance coefficients would, of course, enable a quantitative evaluation of the equilibria involved. However, as it is reasonable to assume that major platinum(II) complexes will exhibit

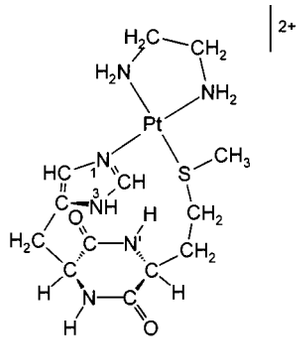

Fig. 2 Structure of $[Pt(en)\{cyclo(-his-met)-\kappa^2N^1,S\}]^{2+}$, the dominant product of the 1:1 $[Pt(en)(H_2O)_2]^{2+}$–cyclo(-his-met-) reaction system for 3.2 < pH < 9.7

similar absorbance coefficients, Fig. 1 and other species distribution diagrams presented in this work should provide an acceptable representation of the pH or time dependence.

Major products were characterized by FAB or ESI-TOF (electrospray-time of flight) mass spectrometry and ^1H and ^{195}Pt NMR spectroscopy. Where necessary, proton resonances were assigned on the basis of H–H correlation spectroscopy (COSY) or H–H total correlation spectroscopy (TOCSY). The methionine and histidine ^1H resonances generally provide unequivocal evidence for the co-ordination of a particular peptide side chain. For instance, a downfield shift from *ca.* δ 2.1 for the free peptide to *ca.* δ 2.5 for a κ*S* complex is characteristic for the δ-CH_3 protons adjacent to the methionine thioether S. The ^1H–^{195}Pt coupling constants (measured at 80 MHz) for H^2 and H^5 in co-ordinated imidazole ring systems correlate with the number of bonds between Pt and the relevant proton. These exhibit equivalent ^3J values of *ca.* 17–20 Hz for N^1 co-ordination. A similar ^3J value is also observed for H^2 in the case of N^3 binding but the $^4J(^1H–^{195}Pt)$ coupling constant for H^5 is now only *ca.* 8–10 Hz. The ^{195}Pt chemical shifts also generally allow a clear distinction between square-planar N_4 and N_3S co-ordination spheres of the Group 10 metal. The δ values for these arrangements lie in the typical respective ranges of −2700 to −2900 and −3000 to −3300.[19]

Cyclo(L-histidyl-L-methionine)

Independent of their composition (*e.g.* 1:1, 1:2 or 2:1), reaction mixtures of $[Pt(en)(H_2O)_2]^{2+}$ with cyclo(-his-met-) afford only one detectable product at pH < 8, namely the macrochelate $[Pt(en)\{cyclo(-his-met-)-\kappa^2N^1,S\}]^{2+}$, the structure of which is depicted in Fig. 2. The formation of this kinetically inert complex is so rapid ($t_{\frac{1}{2}}$ < 1 min) that later addition of NaOH to provide a pH of 10–11 after 15 min leaves the product distribution unchanged. This means that immediate pH adjustment of $[Pt(en)(H_2O)_2]^{2+}$–cyclo(-his-met-) reaction solutions is essential in the determination of the species diagram presented in Fig. 1. Sulfur co-ordination in the dominant κ^2N^1,S complex is confirmed by the downfield shift of the δ-CH_3 protons in the ^1H NMR spectrum (Fig. 3) to δ 2.52, N^1 co-ordination by the equivalence of the $J(^1H–^{195}Pt)$ coupling constants for H^2 and H^5 (Table 1). Both FAB and ESI-TOF mass spectra of a sample of $[Pt(en)\{cyclo(-his-met-)-\kappa^2N^1,S\}][NO_3]_2$ prepared directly in acid solution contain a molecular ion at *m*/*z* 522 corresponding to $[M]^+$. However, the ESI-TOF base peak lies at *m*/*z* 261, corresponding to a doubly charged cation. This peak's isotopic pattern and the absence of molecular ions above $[M + NO_3]^+$ at *m*/*z* 585 confirm the monomeric structure of the $\kappa N^1,S$ complex. Although cyclo(-his-his-) has been shown to chelate both Zn^{2+} and Cu^{2+} through its imidazole rings in solution[20] and the κ^2N^1,N^1 co-ordination mode has been confirmed for $[Cu\{cyclo(-his-his-)\}_2][ClO_4]_2$ in the solid state,[21] no previous example of a cyclo(-his-met-) chelate has, to our knowledge, been reported. In solution, the divalent metal cations Ni^{2+},

Table 1 Proton NMR chemical shifts δ and FAB mass spectral base peaks (*m*/*z*) for (en)Pt^{II} complexes of cyclo(-his-met-)

Proton	κ^2N^1,S	$\kappa^2N'_{met},S$ (I)	$\kappa^2N'_{met},S$ (II)	cyclo(-his-met-)
H^2	8.21 (s), ^3J = 19 Hz	8.71, 8.70 (s)	8.63 (s)	7.72 (s)
H^5	7.12 (s), ^3J = 19 Hz	7.40, 7.34 (s)	7.23 (s)	6.99 (s)
CH_2-β_{his}	3.06 (dd), 3.46 (br)	3.20, 3.35 (dd)	3.16, 3.37 (dd)	3.02, 3.30 (dd)
CH-α_{his}	4.5 (br)	4.36 (dd)	4.53 (dd)	4.42 (dd)
CH-α_{met}	4.13 (dd)	4.03 (d)	4.39 (dd)	4.12 (dd)
CH_2-β_{met}	1.02, 1.57 (br)	0.43, 2.5 (m)	2.06 (m)	1.20, 1.66 (m)
		1.20, 2.5 (m)	2.22 (m)	
CH_2-γ_{met}	2.07 (br)	3.1 (m)	2.6, 3.0 (m)	2.13 (m)
CH_3-δ_{met}	2.52 (s)	2.26, 2.48 (s)	2.40, 2.50 (s)	2.04 (s)
CH_2 of en	2.82 (s)	2.74 (s)	2.75 (s)	
pH*	2.1	1.4	2.9	7.2
FAB (*m*/*z*)	522	522	527*	

* H/D Exchange.

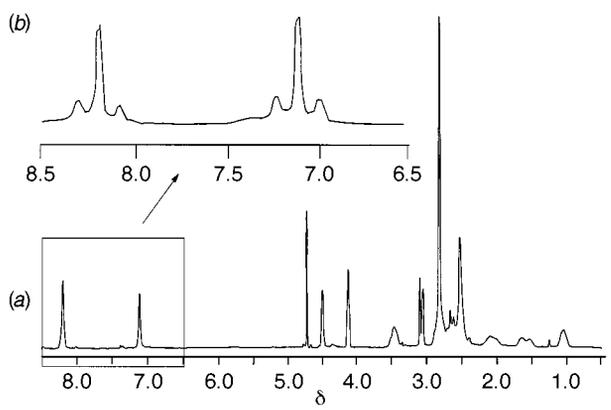

Fig. 3 Proton NMR spectrum of $[Pt(en)\{cyclo(-his-met-)\}]^{2+}$ at pH 2.1: (*a*) at 400 MHz, (*b*) at 80 MHz

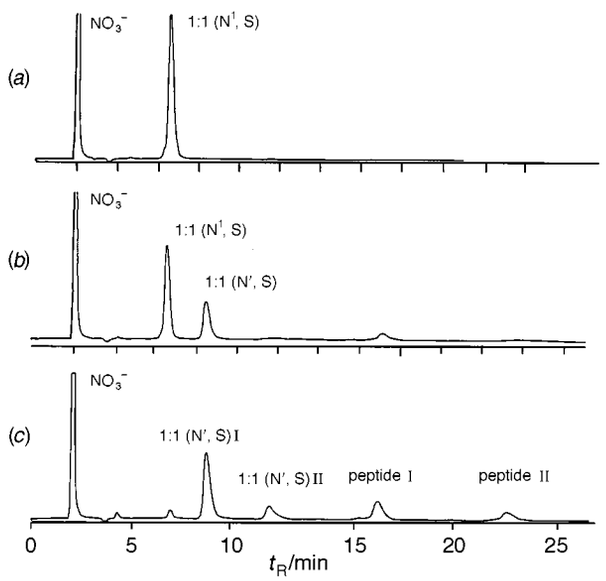

Fig. 4 Chromatograms (mobile phase 96.5% water–3.5% CH_3OH, ion-pairing agent 0.1% pfp, pH 2.1, detection wavelength = 220 nm) for the 1:1 $[Pt(en)(H_2O)_2]^{2+}$–cyclo(-his-met-) reaction system at pH 6.5 (*a*), 9.4 (*b*) and 10.3 (*c*)

Cu^{2+} and Zn^{2+} bind exclusively to imidazole nitrogen atoms[22] and κN^1 co-ordination has been established for the latter cation by X-ray structural analysis for $[Zn\{cyclo(-his-met-)\}_4]SO_4$.[23] Nuclear magnetic resonance investigations[24] indicate that Ag^+ prefers the thioether sulfur in cyclo(-his-met-) and κS co-ordination has been found for polymeric $[Ag\{cyclo(-met-met-)\}]ClO_4$ in the solid state.[25]

Examples of the participation of cisplatin or $[Pt(en)(H_2O)_2]^{2+}$ in chelates have previously been restricted to small thermodynamically favoured five- to seven-membered rings and it has been suggested[8] that involvement of a κS co-ordinated methionine side chain in larger macrocycles should be unlikely. However, our present study demonstrates that in acid solution quantitative formation of the 12-membered chelate ring in $[Pt(en)\{cyclo(-his-met-)\}]^{2+}$ is complete within a number of minutes, thereby indicating that such a κ^2N^1,S co-ordination could be kinetically competitive with other rapid reactions when met and his side chains are present in suitable spacial proximity in peptides and proteins. It seems probable that the apparent preference for the imidazole N^1 site must result from its sterically more open position relative to an S-bound $(en)Pt^{2+}$ fragment. The strength of the Pt–S and Pt–N^1 bonds and the successful shielding of the divalent metal atom from nucleophilic attack provided by the voluminous cyclopeptide (Fig. 2) may be assumed to be responsible for the remarkable kinetic inertness of this complex. However, despite this stability, broad ^1H NMR signals for the CH and CH_2 protons of the met and his side chains (Fig. 3) indicate that the 12-membered macrocycle must exhibit a pronounced degree of conformational flexibility.

A further interesting feature of the $[Pt(en)(H_2O)_2]^{2+}$–cyclo(-his-met-) reaction system is illustrated by the pH-dependent chromatograms presented in Fig. 4. Two new peaks for S-bound complexes with longer retention times can be observed for pH > 8. With the exception of the CH_2-β_{his} resonances, the ^1H NMR signals of two species present in an integral ratio of *ca.* 3:2 in the first additional fraction I exhibit very similar positions (Table 1). As the absence of ^1H–^{195}Pt coupling for the H^2 and H^5 resonances indicates that the imidazole ring cannot be involved in platinum binding, and the ^{195}Pt chemical shifts of δ −3247 and −3294 lie in the typical range for an N_3S co-ordination sphere already registered for the κ^2N^1,S complex (δ −3180), it may reasonably be assumed that κ^2N',S species must be involved. Their formation at pH > 8 will be favoured by the facile deprotonation of the amide nitrogens N′ in alkaline solution. As participation of N'_{his} would lead to the formation of a heavily strained seven-membered chelate ring, it is probable that $\kappa^2N'_{met},S$ species are present in the chromatographic fraction I (N',S) (Fig. 4) with a possible structure being illustrated in Fig. 5(*a*). An N_2SO co-ordination sphere may be ruled out as κO binding by peptide oxygens is only to be expected in acid solution and typical ^{195}Pt chemical shifts[19,26] for such a ligand arrangement lie between δ −2600 and −2700.

The observation of two singlets at δ 2.26 and 2.48 for the CH_3-δ_{met} protons is in accordance with the presence of diastereomers with different configurations at the methionine sulfur. One of the CH_2-β_{met} protons is shifted upfield to δ 0.43, presumably as a result of the adoption of an unusual conform-

Table 2 Proton and ^{195}Pt NMR chemical shifts δ and FAB mass spectral base peaks for complexes separated from the 1:1 $[Pt(en)(H_2O)_2]^{2+}$–his-Hmet reaction system

Proton	κ^2N^1,S	$\kappa^2N'_{met},S$	κ^2N,N^3	κ^2O,S	$(\kappa S)_2$	his-Hmet
H^2	8.23 (s), ^3J = 18 Hz	8.72 (s)	7.89 (s), ^3J = 18 Hz	8.69 (s)	8.69 (s)	8.06 (s)
H^5	7.07 (s), ^3J = 20 Hz	7.45 (s)	7.10 (s), ^4J = 8 Hz	7.46 (s)	7.45 (s)	7.17 (s)
CH_2-β_{his}	3.22, 3.37 (m)	3.07, 3.32 (m)	3.14 (m)	3.45 (m)	3.45 (m)	3.24 (dd)
CH-α_{his}	4.07 (dd)	4.04 (m)	3.72 (dd)	4.37 (m)	4.38 (dd)	4.16 (dd)
CH-α_{met}	3.67 (d)	4.38 (m)	4.42 (dd)	5.60, 5.89 (dd)	4.60 (m)	4.29 (dd)
CH_2-β_{met}	1.43, 1.86 (m)	2.16 (m)	1.98, 2.13 (m)	2.1–2.4 (m)	2.22, 2.38 (m)	1.98, 2.12
CH_2-γ_{met}	2.4, 2.9 (m)	2.6 (m)	2.5 (m)	2.9–3.1 (m)	3.1 (m)	2.52 (m)
CH_3-δ_{met}	2.59 (s)	2.53 (s)	2.08 (s)	2.54 (s)	2.62 (s)	2.12 (s)
CH_2 of en	2.81 (s)	3.07 (m)	2.69 (s)	2.73 (s)	2.87 (s)	
δ (^{195}Pt)	−3219	−3203	−2881		−3767	
pH*	2.5	2.3	1.5	2.1	1.8	6.9
FAB (*m/z*)	542	541	544*	541	827	

* H/D Exchange.

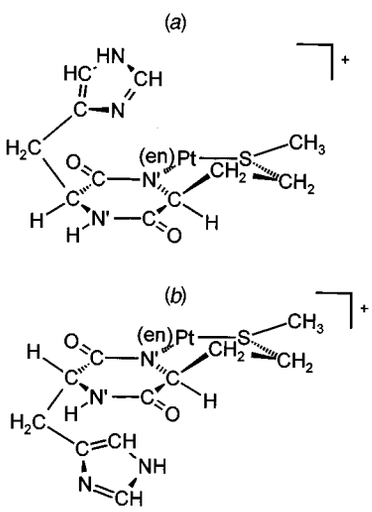

Fig. 5 Possible structures for the $\kappa^2N'_{met},S$ complexes of the chromatographic fractions I and II: (*a*) [Pt(en){cyclo(-L-his-L-met-)-κ^2N',S}]$^{2+}$, (*b*) [Pt(en){cyclo(-D-his-L-met-)-κ^2N',S}]$^{2+}$

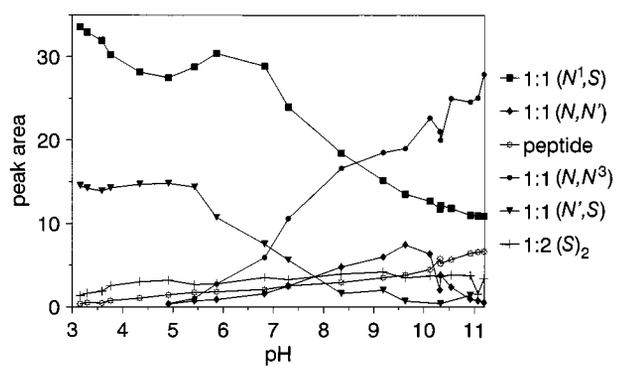

Fig. 6 Species distribution for the 1:1 $[Pt(en)(H_2O)_2]^{2+}$–his-Hmet reaction system after 14 d at 313 K as determined by HPLC (mobile phase 98.5% water–1.5% CH_3OH followed by a gradient step to 94% water–6% CH_3OH after 20 min, ion-pairing reagent 0.1% pfp, pH 2.1, wavelength = 220 nm) for the range 3.2 < pH < 11.2

ation by one of the diastereomers, bringing the relevant proton closer to an electron-rich part of the molecule (*e.g.* the imidazole ring system). For instance a planar [*e.g.* Fig. 5(*a*)] or flagpole-like [20,27] conformation of the histidine side chain involving a boat-shaped central diketopiperazine ring could be stabilized by N–H · · · N hydrogen bonding between en and the free imidazole ring system.

As indicated by the presence of singlets at δ 2.40 and 2.50 for the δ-CH_3 protons of the co-ordinated methionine side chain, diastereomers must also be contained in the second additional complex fraction II of the $[Pt(en)(H_2O)_2]^{2+}$–cyclo(-his-met-) reaction system, collected after a retention time of *ca.* 12 min at pH 10.3 [Fig. 4(*c*)]. Despite the high pH, the imidazole ring is not involved in platinum binding and the similarity of the ^{1}H NMR spectrum to that of fraction I (Table 1) suggests the adoption of a similar $\kappa^2N'_{met},S$ co-ordination mode. The presence of additional chromatographic complex fractions I (t_R = 8.5 min) and II (t_R = 12 min) at higher pH is accompanied by the appearance of a second peptide fraction II with a retention time of 25 min as opposed to 17 min for the original peptide cyclo(-his-met-). These fractions are also observed under similar conditions in the absence of $[Pt(en)(H_2O)_2]^{2+}$. The ESI-TOF mass spectrum affords a mass *m/z* 271 after deuterium exchange for the molecular ions of both peptide fractions. This observation and the similarity of the ^{1}H NMR spectra of both chromatographic peptide fractions suggest that base-catalysed deprotonation of an α-proton, favoured by stabilization of the resulting planar sp^2 α-C atom through mesomeric structures of the diketopiperazine ring, could allow a configuration change on reprotonation, as required under the prevailing conditions for reversed-phase HPLC at pH 2.1. An analogous reprotonation of the $\kappa^2N'_{met},S$ complexes present in solution at high pH should also lead to the appearance of two chromatographic fractions, as is indeed observed. A possible structure of a species [Pt(en){cyclo(-D-his-L-met)-$\kappa^2N'_{met},S$}]$^{2+}$, belonging to the second complex fraction II, is depicted in Fig. 5(*b*). The siting of met and his side chains on opposite sides of the central six-membered ring should prevent an increase in shielding for CH_2-β_{met} protons in close proximity to the electron-rich imidazole ring system. In accordance with this prediction, only downfield shifts are observed for these protons in complex fraction II (Table 1).

L-Histidyl-L-methionine

In view of the remarkable kinetic inertness of the κ^2N^1,S macrochelate (Fig. 2) for the $[Pt(en)(H_2O)_2]^{2+}$–cyclo(-his-met-) reaction system, it was of interest to compare the behaviour of the cyclodipeptide with that of the analogous linear dipeptide his-Hmet, with its increased degree of conformative flexibility. As may be seen in Fig. 6, a κ^2N^1,S macrochelate is once again dominant in acid solution and may be observed over the full pH range 3.2–11.2. However, in this case, $\kappa^2N'_{met},S$ binding is competitive at low pH (3.2–6.8), only to be replaced as an alternative co-ordination mode by the κ^2N (amino),N^3 complex in alkaline solution. Proton and ^{195}Pt NMR chemical shifts for complexes separated from 1:1 $[Pt(en)(H_2O)_2]^{2+}$–his-Hmet reaction solutions by ion-pairing reversed-phase HPLC are presented in Table 2. Structures established on the basis of NMR and mass

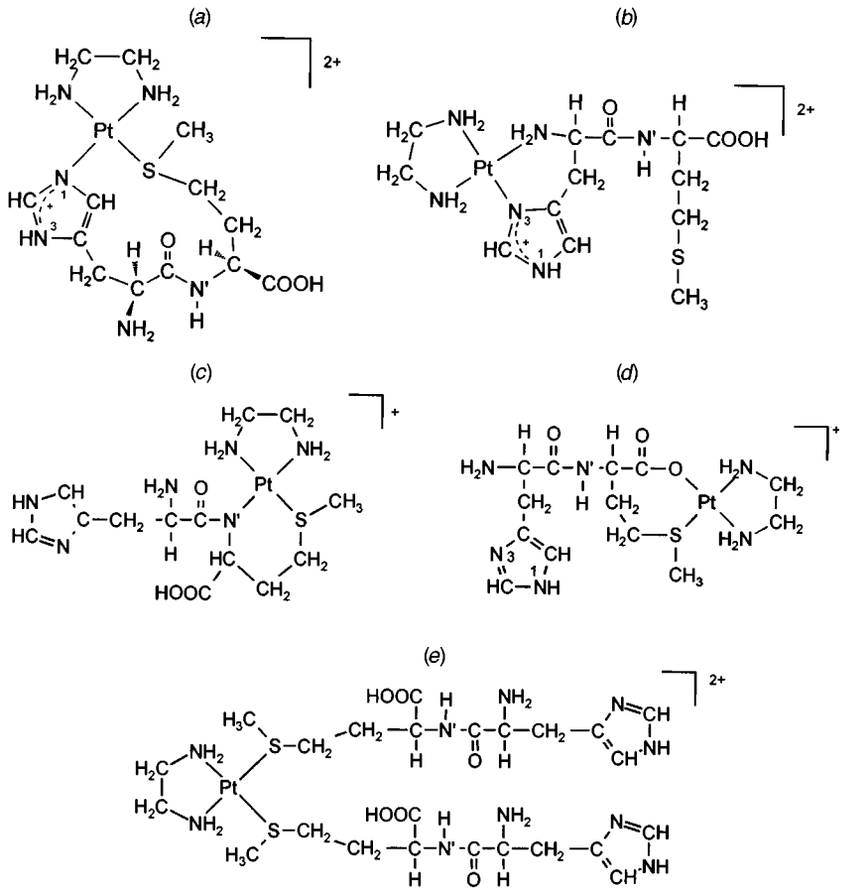

Fig. 7 Structures of platinum(II) complexes separated by HPLC from the 1 : 1 $[Pt(en)(H_2O)_2]^{2+}$–his-Hmet reaction system: (*a*) κ^2N^1,S, (*b*) κ^2N,N^3, (*c*) $\kappa^2N'_{met},S$, (*d*) κ^2O,S, (*e*) $(\kappa S)_2$

spectrometric data are depicted in Fig. 7. The assignment of the second chromatographic peak in alkaline solution to a κ^2N,N'_{met} chelate remains tentative. As for the analogous cyclopeptide, the ESI-TOF mass spectrum of the κ^2N^1,S complex of the linear dipeptide once again exhibits a base peak (*m*/*z* 271) corresponding to a doubly charged macrochelate [Fig. 7(*a*)]. Conformational changes for the 12-membered ring in this complex are slower on the NMR time-scale than for the analogous chelate ring of cyclo(-his-met-), thereby allowing resolution of the fine structure of the his and met CH and CH_2 resonances listed in Table 2. Confirmation for an N_3S environment of Pt^{II} in the competitive S-bound his-Hmet species $\kappa^2N'_{met},S$ in acid solution [Fig. 7(*c*)] is provided by the ^{195}Pt chemical shift of δ −3203.[19] The differing ^1H–^{195}Pt coupling constants for H^2 and H^5 in the major product at pH > 8.5 are in accordance with the imidazole N^3 co-ordination required for the formation of a thermodynamically favoured six-membered κ^2N,N^3 chelate [Fig. 7(*b*)]. Corroborative evidence for this binding pattern is provided by the upfield shift of the CH-α_{his} proton signal to δ 3.72 and the ^{195}Pt chemical shift of δ −2881 typical for an N_4 environment. A strongly retarded minor species [Fig. 8(*c*), $t_R \approx 50$ min] could also be separated from the 1 : 1 $[Pt(en)(H_2O)_2]^{2+}$–his-Hmet reaction system and spectroscopically characterized as the 1 : 2 $(\kappa S)_2$ complex $[Pt(en)(his\text{-}Hmet)_2]^{2+}$, depicted in Fig. 7(*e*). The presence of two his-Hmet ligands is confirmed by the FAB mass spectrometric molecular ion $[M]^+$ at *m*/*z* 827 and the 1 : 2 integral ratio of en to dipeptide in the ^1H NMR spectrum (Table 2). The $(\kappa S)_2$ co-ordination is also established by the ^{195}Pt chemical shift of δ −3767, which lies in the range δ −3600 to −3800 typical for an N_2S_2 environment,[10,19] *e.g.* δ −3757 for $[Pt(en)(amet\text{-}\kappa S)_2]^{2+}$ (amet = *N*-acetylmethionine).[10]

The pH-dependent reversed-phase HPLC separation of products of the 1 : 1 $[Pt(en)(H_2O)_2]^{2+}$–his-Hmet reaction system

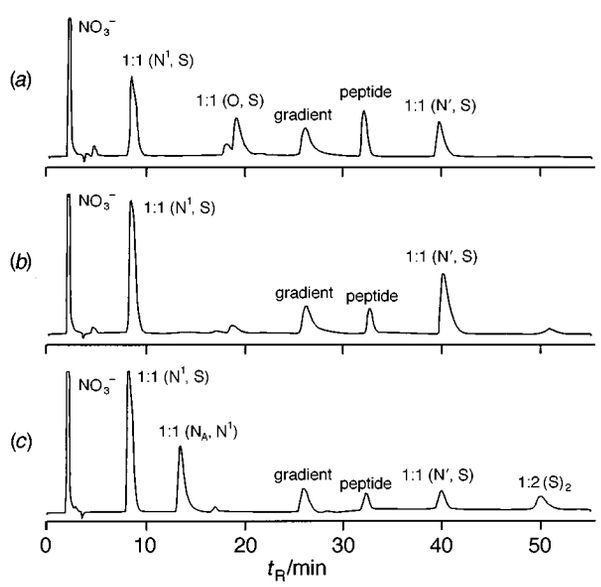

Fig. 8 Chromatograms (mobile phase 99.9% water–0.1% CH_3OH followed by a gradient step to 95.5%–4.5% CH_3OH after 20 min, ion-pairing reagent 0.1% pfp, pH 2.1, wavelength = 220 nm) for the 1 : 1 $[Pt(en)(H_2O)_2]^{2+}$–his-Hmet reaction system after (*a*) 1.28, (*b*) 25 and (*c*) 1500 h. The chromatographic peak for pfp after the gradient step is caused by a temporary partial desorption of the ion-pairing agent

after incubation at 313 K for 14 d indicate a dominance for the κ^2N^1,S macrochelate in acid solution similar though less pronounced than that established for the analogous cyclopeptide. In view of the known kinetic preference of Pt^{II} for methionine S and the established inertness of [Pt(en){cyclo(-his-met-)-

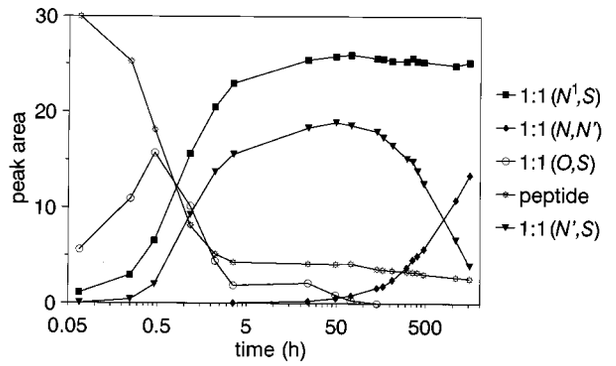

Fig. 9 Time dependence of product formation in the 1:1 $[Pt(en)(H_2O)_2]^{2+}$–his-Hmet reaction mixture as determined by HPLC (conditions as for Fig. 8); pH 4.55 after 14 d at 313 K. Minor species have been omitted for clarity

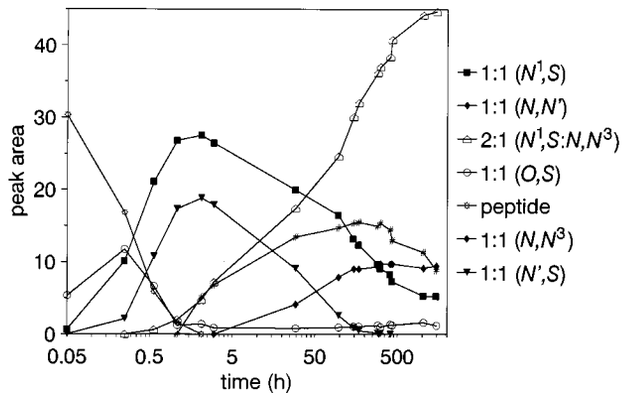

Fig. 10 Time dependence of product formation in the 2:1:1.75 $[Pt(en)(H_2O)_2]^{2+}$–his-Hmet–NaOH reaction mixture as determined by HPLC (conditions as for Fig. 8); pH 6.3 after 14 d at 313 K

$\kappa^2N^1,S\}]^{2+}$, it was of interest to study the time dependence of product formation for the linear dipeptide his-Hmet, which is capable of offering the $\kappa^2N'_{met},S$, κ^2N,N^3 and κ^2N,N'_{met} co-ordination modes (see Figs. 6 and 7), with their thermodynamically favoured smaller five- or six-membered chelate rings as competitive alternatives to κ^2N^1,S macrochelation. Fig. 8 depicts chromatograms registered for the 1:1 $[Pt(en)(H_2O)_2]^{2+}$–his-Hmet reaction mixture after incubation periods of respectively (*a*) 1.28, (*b*) 25 and (*c*) 1500 h. A pH of 4.55 was measured after 14 d (*i.e.* under the prevailing conditions for the species distribution diagram presented in Fig. 6). A gradient step in the composition of the chromatographic mobile phase from 99.9% water–0.1% CH_3OH to 95.5% water–4.5% CH_3OH is necessary to enable the subsequent separation of the strongly retarded $\kappa^2N'_{met},S$ and $(\kappa S)_2$ complexes. This increase in CH_3OH concentration is associated with a temporary partial desorption of the ion-pairing agent from the stationary phase, resulting in the appearance of a chromatographic peak for pfp (detection wavelength 220 nm) after the gradient step (Fig. 8).

The time dependence of species distribution in the 1:1 $[Pt(en)(H_2O)_2]^{2+}$–his-Hmet reaction system presented in Fig. 9 indicates that an intermediate product, presumably a κ^2O,S chelate [Fig. 7(*d*)], is formed very rapidly, only to convert into the major species at pH 4–5, namely κ^2N^1,S and $\kappa^2N'_{met},S$ co-ordinated complexes, within 5 h. Although the separated quantity of this intermediate did not allow the registration of a satisfactory ^{195}Pt NMR spectrum, strong evidence for κ^2O,S chelation is provided by the pronounced downfield shift of the CH-α_{met} proton adjacent to the co-ordinated carboxylate oxygen. Chemical shifts of δ 5.33 and 5.58 have been reported by Appleton *et al.*[19] for the α-proton in *cis*-$[Pt(NH_3)_2(Hmet\text{-}\kappa^2O,S)]^{2+}$, values similar to resonance positions of δ 5.60 and 5.89 recorded for CH-α_{met} in the diastereomers of $[Pt(en)(his\text{-}Hmet\text{-}\kappa^2O,S)]^{2+}$ (Table 2).[11] Upon reaching a quasi-stationary state after *ca.* 50 h, the $\kappa^2N'_{met},S$ complex slowly converts into the presumably thermodynamically more stable κ^2N,N'_{met} five-membered chelate. The time-dependent species distribution allows an elucidation of the reaction pathway leading to this final N_4 environment. Although not involved in the ultimate co-ordination sphere the methionine S plays a crucial role as an anchor in the initial κ^2O,S chelate, thereby enabling the slow formation of $Pt–N'_{met}$ bonds by metallation of the neighbouring amide nitrogen. Subsequent replacement of the initially kinetically favoured sulfur atom by a terminal amino nitrogen atom leads to the even slower increase in concentration for $[Pt(en)(his\text{-}met\text{-}\kappa^2N,N'_{met})]^+$ after 50 h. Though formation of the 12-membered macrochelate is less rapid for the linear dipeptide his-Hmet than for the analogous cyclopeptide, an analogous kinetic inertness is exhibited by both κ^2N^1,S complexes in acid solution. However, at pH > 6 the concentration of the macrochelate declines slowly after incubation of the $[Pt(en)(H_2O)_2]^{2+}$–his-Hmet reaction system for *ca.* 300 h at 313 K, owing to formation of the thermodynamically preferred κ^2N,N^3 six-membered chelate.

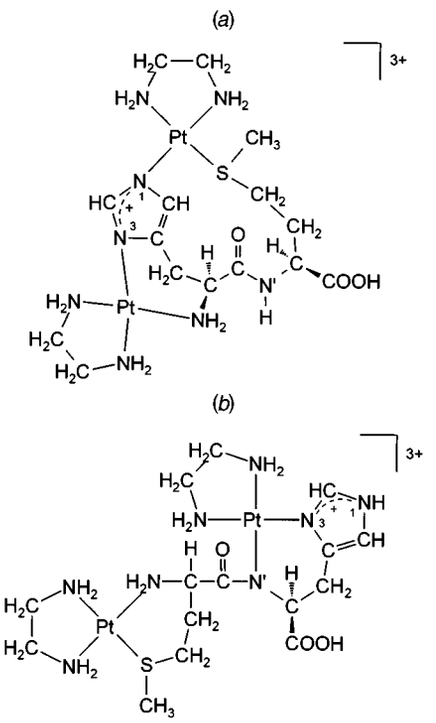

Fig. 11 Structures of the 2:1 complexes (*a*) $[\{Pt(en)\}_2(hisH_{-1}\text{-}Hmet\text{-}1\kappa^2N,N^3:2\kappa^2N^1,S)]^{3+}$ and (*b*) $[\{Pt(en)\}_2(met\text{-}his\text{-}1\kappa^2N,S:2\kappa^2N'_{his},N^3)]^{3+}$

The methionine sulfur also behaves as an initial anchor for subsequent interaction between $(en)Pt^{2+}$ and the dipeptide in the 2:1:1.75 $[Pt(en)(H_2O)_2]^{2+}$–his-Hmet–NaOH reaction mixture, the time-dependent product distribution of which is depicted in Fig. 10. Indeed, the first two reaction steps, in which rapid κ^2O,S co-ordination is followed by formation of the κ^2N^1,S macrochelate or the $\kappa^2N'_{met},S$ species, are identical to those established for a 1:1 $(en)Pt^{2+}$:his-Hmet ratio. However, for the 2:1 reaction system, these complexes reach their concentration maxima after *ca.* 3 h and then steadily decline in importance. The free histidine nitrogen atoms N (amino) and N^3 in the 12-membered macrochelate co-ordinate a second $(en)Pt^{II}$ fragment in a third reaction step to afford the $1\kappa^2N,N^3:2\kappa^2N^1,S$ 2:1 complex [Fig. 11(*a*)], which can first be detected after *ca.* 2 h and subsequently becomes the dominant species after *ca.* 40 h. As the κ^2N^1,S and $\kappa^2N'_{met},S$ complexes decline in importance, slow formation of the thermodynamically favoured κ^2N,N^3 and κ^2N,N'_{met} chelates is registered. Both the FAB mass spectrum, with its molecular ion at *m*/*z* 800, and the ^1H (Fig. 12) and ^{195}Pt NMR spectra are in accordance with the formulation of the thermodynamically dominant

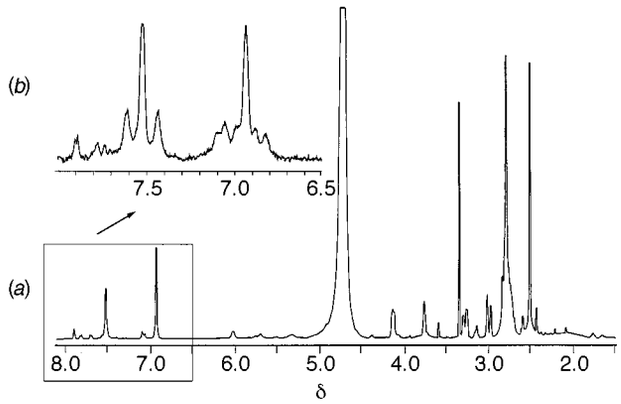

Fig. 12 Proton NMR spectrum of $[\{Pt(en)\}_2(hisH_{-1}\text{-Hmet-}1\kappa^2N,N^3:2\kappa^2N^1,S)]^{3+}$ at pH 1.5: (*a*) at 400 MHz, (*b*) at 80 MHz

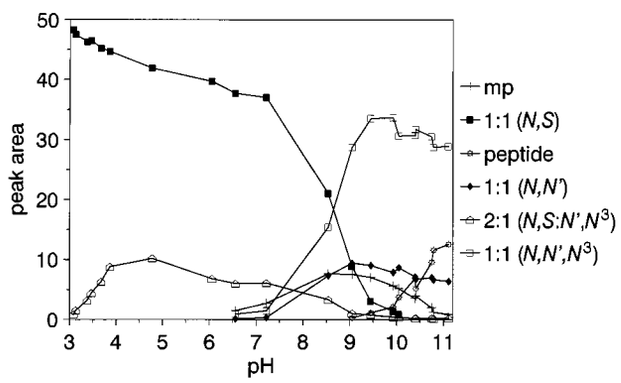

Fig. 13 Species distribution for the 1:1 $[Pt(en)(H_2O)_2]^{2+}$–met-Hhis reaction system after 14 d at 313 K as determined by HPLC (mobile phase 100% water followed by gradient step to 80% water–20% CH_3OH after 18 min, ion-pairing agent 0.04% pfp, pH 2.1, wavelength 220 nm) for the range 3.0 < pH < 11.2; mp = minor product

species as $[\{Pt(en)\}_2(hisH_{-1}\text{-Hmet-}1\kappa^2N,N^3:2\kappa^2N^1,S)]^{3+}$. Co-ordination of two (en)Pt^{II} fragments by the linear dipeptide is confirmed by the observation of ^1H–^{195}Pt coupling between H^5 and Pt atoms at both possible imidazole binding sites. Respective ^3J and ^4J values are 19 and 8.5 Hz. Whereas one of the two ^{195}Pt resonances for this complex lies in the typical range for N_3S co-ordination (δ −3181), the second δ −2879 is characteristic for an N_4 environment, as provided by κ^2N,N^3 chelation.

L-Methionyl-L-histidine

We have previously reported the dominance of κ^2N,S chelation at pH < 8.7 for peptides such as met-Hgly and met-gly-Hgly with N-terminal methionine residues.[10] At higher pH the κ^2N,N'_{gly} co-ordination mode is preferred. In view of the kinetic inertness established for the κ^2N^1,S macrochelate of both cyclo(-his-met-) and his-Hmet, it was of interest to establish whether thioether-S anchoring of the (en)Pt^{II} fragment would also be capable of providing a reaction pathway to an imidazole-co-ordinated 1:1 complex for met-Hhis. As participation in a kinetically favoured κ^2O,S six-membered chelate is no longer possible for the N-terminal methionine side chain, facile formation of the thermodynamically favoured κ^2N,S complex might be expected to prevent macrochelation for this dipeptide. The pH-dependent species distribution diagram (Fig. 13) determined by reversed-phase HPLC for the 1:1 $[Pt(en)(H_2O)_2]^{2+}$–met-Hhis reaction system after incubation at 313 K for 14 d indicates that this is indeed the case. The complex $[Pt(en)(met\text{-}Hhis\text{-}\kappa^2N,S)]^{2+}$ dominates for pH < 8.7 and is replaced by $[Pt(en\text{-}\kappa N)(met\text{-}his\text{-}\kappa^3N,N'_{his},N^3)]^{+}$ at higher pH. Fig. 13 is, in fact, very similar to the species distribution diagram

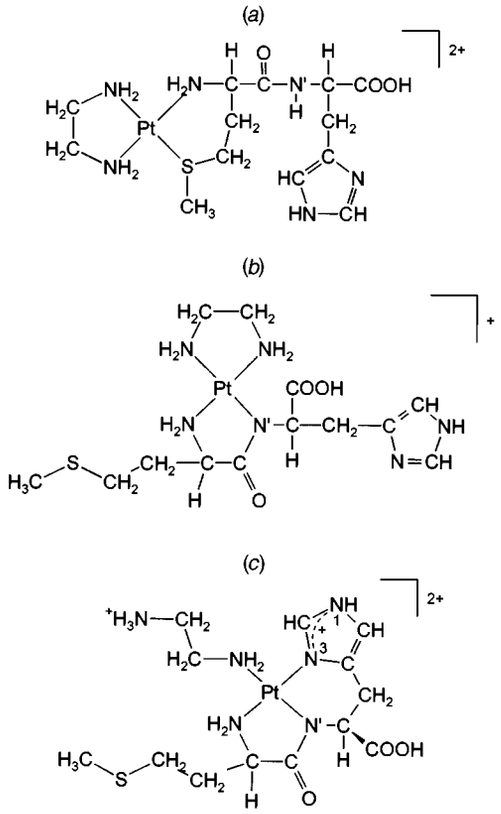

Fig. 14 Structures of the platinum(II) complexes separated by HPLC from the 1:1 $[Pt(en)(H_2O)_2]^{2+}$–met-Hhis reaction system: (*a*) κ^2N,S, (*b*) κ^2N,N'_{his}, (*c*) κ^3N,N'_{his},N^3

Table 3 Proton and ^{195}Pt NMR chemical shifts δ and FAB mass spectral base peaks for 2:1 complexes of (en)Pt^{II} with dipeptides his-Hmet and met-Hhis

Proton	his-Hmet $1\kappa^2N,N^3:2\kappa^2N^1,S$	met-Hhis $1\kappa^2N,S:2\kappa^2N'_{his},N^3$
H^2	7.52 (s) [$J(^1H$–$^{195}Pt)$ 14 Hz]	7.87 (s) [$J(^1H$–$^{195}Pt)$ 17 Hz]
H^5	6.94 (s) [$J(^1H$–$^{195}Pt)$ 8.5, 19 Hz]	7.07 (s) [$J(^1H$–$^{195}Pt)$ 8 Hz]
CH_2-β_{his}	3.0 (d), 3.27 (dd)	3.3 (m)
CH-α_{his}	3.76 (m)	3.95 (dd)
CH-α_{met}	4.13 (m)	3.62 (dd)
CH_2-β_{met}	1.8–2.3 (m)	1.80, 2.09 (m)
CH_2-γ_{met}	2.7–2.8 (m)	3.0 (m)
CH_3-δ_{met}	2.51 (s)	2.53, 2.58 (s)
CH_2 of en	2.79 (s)	2.77 (m)
δ (^{195}Pt)	−2879, −3181	−2779, −3331
pH*	1.5	4.9
FAB (*m*/*z*)	800*	793

* H/D Exchange.

obtained for met-Hgly,[10] with the major difference being that only κ^2N,N'_{gly} chelation is possible for the glycine-containing dipeptide at pH > 8.7, owing to its lack of a second amino acid residue with a co-ordinating side chain. As will be discussed later, the analogous κ^2N,N'_{his} chelate is a required intermediate product on the reaction pathway to the met-Hhis κ^3N,N'_{his},N^3 complex and is present as a minor species in Fig. 13. The presence of the imidazole-containing side chain in met-Hhis also leads to a second important difference in the species distribution diagrams for the 1:1 reaction of $[Pt(en)(H_2O)_2]^{2+}$ with respectively met-Hhis and met-Hgly, namely the formation of a novel 2:1 complex $[\{Pt(en)\}_2(met\text{-}his\text{-}1\kappa^2N,S:2\kappa^2N'_{his},N^3)]^{3+}$ by the former dipeptide in acid solution (Fig. 13). Proton NMR data

Table 4 Proton NMR chemical shifts δ and FAB mass spectral base peaks for complexes separated from the 1:1 $[Pt(en)(H_2O)_2]^{2+}$–met-Hhis reaction system

Proton	κ^2N,S	κ^2N,N'_{his}	κ^3N,N'_{his},N^3	met-Hhis
H^2	8.60 (s)	8.60 (s)	8.02 (s), ^3J = 18 Hz	8.26 (s)
H^5	7.29 (s)	7.39 (s)	7.13 (s), ^4J = 10 Hz	7.16 (s)
CH_2-β_{his}	3.27, 3.34 (dd)	2.9, 3.25 (dd)	3.32 (m)	3.18 (m)
CH-α_{his}	4.55 (dd)	4.82 (dd)	4.40 (dd)	4.47 (dd)
CH-α_{met}	3.66, 3.75 (dd)	3.68 (dd)	3.83 (dd)	4.04 (t)
CH_2-β_{met}	2.21, 2.3 (m)	1.87, 1.96 (m)	1.98, 2.21 (m)	2.13 (m)
CH_2-γ_{met}	3.05 (m)	2.53 (m)	2.72 (m)	2.58 (m)
CH_3-δ_{met}	2.56 (s)	2.11 (s)	2.14 (s)	2.11 (s)
CH_2 of en	2.76 (s)	2.63 (m)	2.95 (d), 3.05 (m)	
pH*	2.9	2.9	3.0	6.7
FAB (*m*/*z*)	541	541	541	

are presented for this complex and the 1:1 species of the $[Pt(en)(H_2O)_2]^{2+}$–met-Hhis reaction system in respectively Tables 3 and 4. Apposite structures are shown in Figs. 11(*b*) and 14(*a*)–14(*c*). The dominant species $[Pt(en)(met\text{-}Hhis\text{-}\kappa^2N,S)]^{2+}$ and $[\{Pt(en)\}_2(met\text{-}his\text{-}1\kappa^2N,S:2\kappa^2N'_{his},N^3)]^{3+}$ were prepared directly, at the appropriate molar ratio and respective pH* values of 2.9 and 4.9, for subsequent NMR studies. In contrast, the κ^2N,N'_{his} and κ^3N,N'_{his},N^3 complexes were separated by reversed-phase HPLC at pH 10.0 from the incubated $[Pt(en)(H_2O)_2]^{2+}$–met-Hhis reaction mixture. As previously reported for met-Hgly and met-gly-Hgly,[10] thioether co-ordination is confirmed for the κ^2N,S complex by the marked downfield shifts of the methionine γ- and δ-protons, N (amino) co-ordination by the upfield shift of CH-α_{met}, the α-proton at the N-terminal end of the dipeptide met-Hhis. An effectively unchanged position for the CH_3-δ_{met} protons rules out thioether co-ordination in the remaining 1:1 complexes in Table 4, for which the pronounced shift of CH-α_{met} to higher frequency once again indicates N (amino) binding. Conclusive evidence for the monodentate κ*N* en required by the κ^3N,N'_{his},N^3 complex [Fig. 14(*c*)] is provided by the appearance of resonances at δ 2.95 and 3.05, which can be assigned to CH_2 protons adjacent to respectively co-ordinated and non-co-ordinated N atoms. Participation of imidazole N^3 in a six-membered $\kappa^2N'_{his},N^3$ chelate is confirmed by the strikingly different ^1H–^{195}Pt coupling constants, with that of H^5 (10 Hz) being characteristic for a ^4J value.

An analogous cleavage of a Pt–N (en) bond has also been reported for the 1:1 $[Pt(en)(H_2O)_2]^{2+}$–gly-Hmet reaction system, leading to the formation of $[Pt(Hen\text{-}\kappa N)(gly\text{-}met\text{-}\kappa^3N,N'_{met},S)]^{2+}$, in which the O-terminal side chain is once again involved in platinum co-ordination,[10] as has also recently been observed in a palladium(II) complex of gly-Hmet and 9-methylguanine.[28] However, in the case of gly-Hmet the high *trans* effect of the methionine sulfur in the intermediate product $[Pt(en)(gly\text{-}met\text{-}\kappa^2N'_{met},S)]^+$ can be assumed to labilize the opposite Pt–N (en) bond, thereby favouring the adoption of a tridentate κ^3N,N'_{met},S binding pattern by the glycine-containing dipeptide. A comparable reaction pathway for met-Hhis would require an intermediate with $\kappa^2N'_{his},N^3$ co-ordination, a species not detected in the range $3 < pH < 11$ after incubation of the reaction mixture at 313 K for 14 d.

Chromatographic time-dependent analyses of various $[Pt(en)(H_2O)_2]^{2+}$–met-Hhis reaction mixtures provide an insight into kinetic and thermodynamic aspects of intramolecular competition between the methione and histidine side chains in this linear dipeptide. After rapid formation, the concentration of the dominant κ^2N,S chelate remains effectively constant in acid solution over 500 h (Fig. 15). At the higher pH 9.6, co-ordination reactions of the dipeptide proceed at a much slower velocity, as indicated by the presence of a significant concentration of the bioligand at the close of the time-dependent

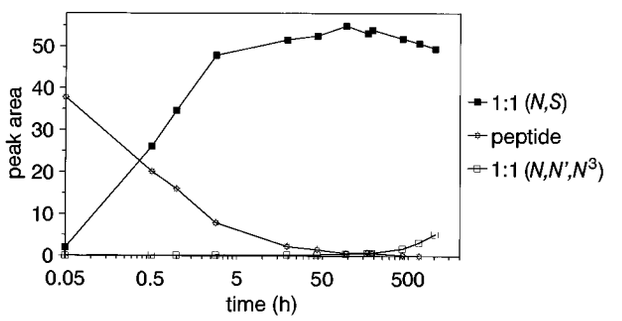

Fig. 15 Time dependence of product formation in the 1:1:0.5 $[Pt(en)(H_2O)_2]^{2+}$–met-Hhis–NaOH reaction mixture as determined by HPLC (conditions as for Fig. 13); pH 6.0 after incubation at 313 K for 14 d. Minor species have been omitted for clarity

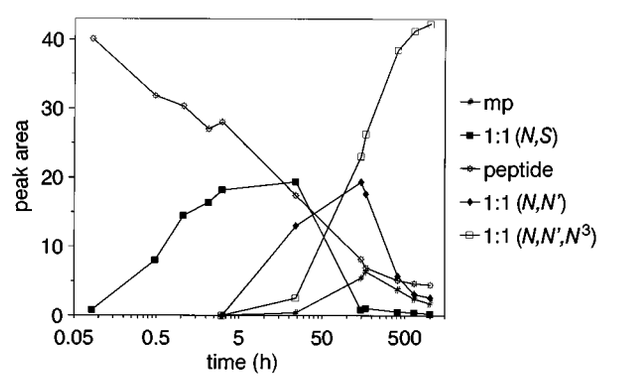

Fig. 16 Time dependence of product formation in the 1:1:2.5 $[Pt(en)(H_2O)_2]^{2+}$–met-Hhis–NaOH reaction mixture as determined by HPLC (conditions as for Fig. 13); pH 9.6 after 14 d at 313 K; mp = minor product

analysis depicted in Fig. 16. Formation of the κ^3N,N'_{his},N^3 complex involves three reaction steps. The kinetic preference of $(en)Pt^{II}$ for the methionine S atom leads to an initial relatively rapid κ^2N,S chelation. An anchoring role is now adopted by the amino N atom, the co-ordination of which accelerates the metallation of the adjacent amide N'_{his} to provide the κ^2N,N'_{his} chelate as a second intermediate product. The concentration of this species reaches a maximum after *ca.* 100 h and then declines as cleavage of the Pt–N (en) bond *trans* to the amino N atom enables the adoption of a tridentate κ^3N,N'_{his},N^3 co-ordination mode in the final product. It is apparent from this reaction pathway that a pronounced *trans* effect, as discussed[10] for $[Pt(en)(gly\text{-}met\text{-}\kappa^2N'_{met},S)]^+$, is not an essential prerequisite for Pt–N (en) cleavage. The driving force behind the final reaction step must be provided by the increased strength of the Pt–N^3 bond to a *softer* aromatic nitrogen and the thermodynamic advantage of the bis-chelate co-ordination mode.

Table 5 The HPLC conditions for semipreparative separation of platinum(II) complexes after incubation of $[Pt(en)(D_2O)_2]^{2+}$ with dipeptides at 313 K for 14 d

Molar ratio Pt^{II} : peptide	Equivalents of NaOH	pH* (after 14 d)	% CH_3OH in mobile phase: initial	final	Gradient time (min)	% (v/v) pfp	t_R[a]/min	Co-ordination mode
cyclo(-his-met-) 2:1	3.5	9.9	3	3	—	0.1	8.5	$\kappa^2N'_{met},S$ (I)
							12	$\kappa^2N'_{met},S$ (II)
his-Hmet 1:1	−1.0[b]	3.5	5	15	18	0.1	8.5	κ^2N^1,S
							19	κ^2O,S
							41	$\kappa^2N'_{met},S$
							51	$(\kappa S)_2$
his-Hmet 1:1	0.75	5.0	0	15	6	0.1	8.5	κ^2N^1,S
							40	κ^2N,N^3
his-Hmet 2:1	1.5	4.5	5	15	18	0.1	16	$1\kappa^2N,N^3:2\kappa^2N^1,S$
met-Hhis 1:1	2.0	10.0	0	20	9	0.04	14.5	κ^2N,N'_{his}
							32	κ^3N,N'_{his},N^3

[a] Analytical separations. [b] Equivalents of HNO_3.

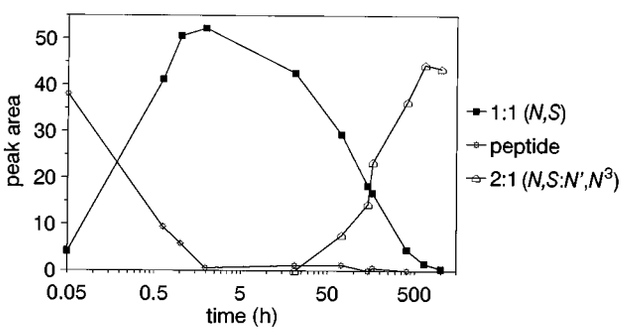

Fig. 17 Time dependence of product formation in the 2:1:1.5 $[Pt(en)(H_2O)_2]^{2+}$–met-Hhis–NaOH reaction mixture as determined by HPLC (conditions as for Fig. 13); pH 5.2 after incubation for 14 d at 313 K

As already observed for his-Hmet, co-ordination of two $(en)Pt^{II}$ fragments is a very slow procedure. After rapid formation of the κ^2N,S chelate, the presence of the 2:1 $1\kappa^2N,S:2\kappa^2N'_{his},N^3$ complex [Fig. 11(*b*)] can first be detected by HPLC for the 2:1 $[Pt(en)(H_2O)_2]^{2+}$–met-Hhis reaction mixture after 3 d (Fig. 17). The formation of the dinuclear complex is effectively complete after 600 h. The $\kappa^2N'_{his},N^3$ co-ordination can be achieved for the second $(en)Pt^{II}$ fragment without bond cleavage in the κ^2N,S intermediate, and its adoption is confirmed by the ^1H and ^{195}Pt NMR data presented in Table 3.

Conclusion

Our present studies on dipeptides confirm the kinetic preference of Pt^{II} for methionine S, which after rapid co-ordination adopts an anchoring role enabling the formation of 12-membered κ^2N^1,S macrochelates when met is not N-terminal. The unusually large chelate ring in $[Pt(en)(his\text{-}Hmet\text{-}\kappa^2N^1,S)]^{2+}$ exhibits a remarkable long-term kinetic stability, even in alkaline solution (pH 7–10) for which κ^2N,N^3 or κ^2N,N'_{met} complexes involving the terminal amino nitrogen are thermodynamically more stable. In view of the fact that platinum is known to exhibit an *in vivo* half-life of several days after administration of cisplatin,[29] our findings suggest that κ^2N^1,S macrochelation by oligopeptides or proteins should not be neglected when reaction pathways are considered for the anticancer drug. Our time-dependent HPLC analyses of the reaction of $[Pt(en)(H_2O)_2]^{2+}$ with the dipeptides his-Hmet and met-Hhis indicate that positional changes required for the conversion of kinetically favoured S-bound species into thermodynamically N-bound complexes are very slow and may not be complete after incubation at 313 K for 500 h. This time-scale appears to have been underestimated in past investigations. The reaction pathways for such transformations involve consecutive chelate formation in which at least one of the dipeptide donor atoms exhibits an anchoring role.

Experimental

Materials

The complex $[PtCl_2(en)]$ was prepared in accordance with literature procedures.[30] The dipeptides cyclo(-his-met-), his-Hmet and met-Hhis were synthesized by Dr. Kalbacher of the Medizinisch-Naturwissenschaftliches Forschungszentrum of the University of Tübingen and used as received. HPLC-Grade methanol and acetonitrile were from J. T. Baker and Merck, pentafluoropropionic acid from Fluka or Aldrich. Stock solutions (4 mmol dm^{-3}) of $[Pt(en)(H_2O)_2][NO_3]_2$ for analytical HPLC were prepared by stirring an aqueous mixture of $[PtCl_2(en)]$ with the required equivalent of $AgNO_3$ (1:1.96) for 24 h in the dark followed by centrifugation of the AgCl precipitate. Solutions (50–200 mmol dm^{-3}) of $[Pt(en)(D_2O)_2][NO_3]_2$ for semipreparative HPLC and NMR investigations were obtained by an analogous procedure in D_2O solution.

HPLC

The following equipment was employed for analytical and semipreparative separations: Merck L-6200A pump, Rheodyne 7125 sample injector, Merck L-4250 variable-wavelength UV/VIS detector. Some isocratic separations were performed with a Knauer 64 pump, A0258 sample injector and a Merck L-4000A UV detector. Integration and evaluation were carried out with Knauer Eurochrom 2000 software. Reversed-phase columns (25 × 0.4 cm inside diameter) packed with Nucleosil 100-C_{18} (5 μm, Macherey–Nagel) were employed for analytical separations. Semipreparative work was carried out on 25 × 2 cm inside diameter reversed-phase columns (Nucleosil 100-C_{18}, 10 μm). Analytical (0.8 mmol dm^{-3} per equivalent) and semipreparative (15 mmol dm^{-3} per equivalent) reaction solutions were prepared at required Pt^{II} : dipeptide molar ratios (1:1, 2:1). The initial pH was adjusted by addition of 0.1 mol dm^{-3} NaOH or HNO_3 and the solutions were incubated for 14 d at 313 K. After registration of the final pH, such solutions were held at 277 K prior to HPLC separation. Samples were run isocratically or with a one-step gradient (6–20 min) using 80–100% water–20–0% methanol as the mobile phase (pH 2.1 ± 0.1) in the presence of 0.04–0.1% (v/v) of pfp. Peak detection was performed at 220 mm. Semipreparative fractions were united from 7–14 separations and the solvent removed under vacuum to yield oily residues. These were treated with diethyl ether, which was sub-

sequently removed to afford the products as powders. Their purity was monitored by analytical HPLC traces and NMR spectroscopy. The HPLC conditions for complexes separated in this manner are listed in Table 5. The dominant products $[Pt(en)\{cyclo(\text{-}his\text{-}met\text{-})\text{-}\kappa^2N^1,S\}]^{2+}$, $[Pt(en)(met\text{-}Hhis\text{-}\kappa^2N,S)]^{2+}$ and $[\{Pt(en)\}_2(met\text{-}his\text{-}1\kappa^2N,S:2\kappa^2N'_{his},N^3)]^{3+}$ were prepared directly for NMR and FAB mass spectral measurements by reaction of $[Pt(en)(D_2O)_2]^{2+}$ with the appropriate dipeptide in D_2O at respective pH* values of 2.1, 2.9 and 4.9.

Mass spectral and NMR measurements

The FAB mass spectra were recorded on a Fisons VG Autospec instrument employing 3-nitrobenzyl alcohol as the matrix. In some cases samples were prepared in D_2O leading to H/D exchange as flagged in Tables 1–4. The ESI-TOF mass spectral measurements were performed by Dr. A. Kraft (University of Gießen). The NMR spectra were recorded at 297 K on a Bruker DRX 400 or WP 80 spectrometer using 5 mm tubes and D_2O as solvent. The chemical shift references were as follows: ^1H, sodium 3-(trimethylsilyl)tetradeuteriopropionate (δ 0.0); ^{195}Pt, saturated $K_2[PtCl_4]$–1 mol dm^{-3} NaCl (external) with δ −1628. pH* Values of solutions in NMR tubes were registered with a micro glass electrode (Hamilton spintrode 238100, length 180 mm).

References

1 S. E. Sherman and S. J. Lippard, *Chem. Rev.*, 1987, **87**, 1153.
2 N. Farrell, *Transition Metal Complexes as Drugs and Chemotherapeutic Agents*, Kluwer Academic Press, Dordrecht, 1989.
3 T. G. Appleton, J. W. Connor, J. R. Hall and P. D. Prenzler, *Inorg. Chem.*, 1989, **28**, 2030.
4 R. F. Borch and M. E. Pleasants, *Proc. Natl. Acad. Sci. USA*, 1979, **76**, 6611.
5 C. M. Riley, L. A. Sternson, A. J. Repta and S. A. Slyter, *Anal. Biochem.*, 1983, **130**, 203.
6 S. S. G. E. van Boom and J. Reedijk, *J. Chem. Soc.*, *Chem. Commun.*, 1993, 1397.
7 K. J. Barnham, M. I. Djuran, P. d. S. Murdoch and P. J. Sadler, *J. Chem. Soc.*, *Chem. Commun.*, 1994, 721.
8 K. J. Barnham, M. I. Djuran, P. d. S. Murdoch, J. D. Ranford and P. J. Sadler, *J. Chem. Soc.*, *Dalton Trans.*, 1995, 3721.
9 P. M. Deegan, I. S. Pratt and M. P. Ryan, *Toxicology*, 1994, **89**, 1.
10 A. F. M. Siebert and W. S. Sheldrick, *J. Chem. Soc.*, *Dalton Trans.*, 1997, 385.
11 Z. Guo, T. W. Hambley, P. d. S. Murdoch, P. J. Sadler and U. Frey, *J. Chem. Soc.*, *Dalton Trans.*, 1997, 469.
12 M. Wienken, E. Zangrando, L. Randaccio, S. Menzer and B. Lippert, *J. Chem. Soc.*, *Dalton Trans.*, 1993, 3349.
13 Y. Kojima, K. Hirotsu, T. Yamashita and T. Miwa, *Bull. Chem. Soc. Jpn.*, 1985, **58**, 1894.
14 T. G. Appleton, F. J. Pesch, M. Wienken, S. Menzer and B. Lippert, *Inorg. Chem.*, 1992, **31**, 4410.
15 V. Aletras, N. Hadjiliadis, A. Lymberopoulou-Karaliota, I. Rombeck and B. Lippert, *Inorg. Chim. Acta*, 1994, **227**, 17; I. Sovago, A. Kiss and B. Lippert, *J. Chem. Soc.*, *Dalton Trans.*, 1995, 489.
16 T. N. Parac and N. M. Kostic, *J. Am. Chem. Soc.*, 1996, **118**, 51, 5946.
17 E. L. M. Lempers and J. Reedijk, *Adv. Inorg. Chem.*, 1991, **37**, 175.
18 A. F. M. Siebert, C. D. W. Fröhling and W. S. Sheldrick, *J. Chromatogr. A*, 1997, **761**, 115.
19 T. G. Appleton, J. W. Connor and J. R. Hall, *Inorg. Chem.*, 1988, **27**, 130.
20 Y. Kojima, *Chem. Lett.*, 1981, 61; S. Kubota and J. T. Yang, *Proc. Natl. Acad. Sci. USA*, 1984, **81**, 3283; Y. Kojima, T. Yamashita, S. Nishide, K. Hirotsu and T. Higuchi, *Bull. Chem. Soc. Jpn.*, 1985, **58**, 409; G. Arena, R. P. Bonomo, G. Impellizzeri, R. M. Izatt, J. D. Lamb and E. Rizzarelli, *Inorg. Chem.*, 1987, **26**, 795; G. Arena, G. Impellizzeri, G. Maccarrone, G. Pappalardo and E. Rizzarelli, *J. Chem. Soc.*, *Dalton Trans.*, 1994, 1227.
21 F. Hori, Y. Kojima, K. Matsumoto, S. Ooi and H. Kuroya, *Bull. Chem. Soc. Jpn.*, 1979, **52**, 1076.
22 Y. Kojima, N. Ishio and T. Yamashita, *Bull. Chem. Soc. Jpn.*, 1985, **58**, 759.
23 Y. Kojima, N. Ishio, T. Yamashita and K. Hirotsu, *Chem. Lett.*, 1983, 1365.
24 Y. Kojima, T. Yamashita, Y. Ishino, T. Hirashima and T. Miwa, *Bull. Chem. Soc. Jpn.*, 1983, **56**, 3841.
25 Y. Kojima, T. Yamashita, Y. Ishino, T. Hirashima and K. Hirotsu, *Chem. Lett.*, 1983, 453.
26 K. J. Barnham, M. I. Djuran, P. d. S. Murdoch, J. D. Ranford and P. J. Sadler, *Inorg. Chem.*, 1996, **35**, 1065.
27 G. Arena, R. P. Bonomo, G. Impellizzeri, R. M. Izatt, J. D. Lamb and E. Rizzarelli, *Inorg. Chem.*, 1987, **26**, 795.
28 M. Wienken, A. Kiss, J. Sóvágó, E. C. Fusch and B. Lippert, *J. Chem. Soc.*, *Dalton Trans.*, 1997, 563.
29 A. W. Prestayko, in *Cisplatin, Current Status and New Developments*, eds. A. W. Prestayko, S. T. Crooke and S. K. Carter, Academic Press, London, 1980, p. 2.
30 L. F. Heneghan and J. C. Bailar, jun., *J. Am. Chem. Soc.*, 1953, **75**, 1840; F. Basolo, J. C. Bailar, jun. and B. R. Tarr, *J. Am. Chem. Soc.*, 1950, **72**, 2433.

Received 9*th June* 1997; *Paper* 7/04002D